MOLECULAR AND CELLULAR BIOLOGY, Jan. 1992, p. 368–378
0270-7306/92/010368-11$02.00/0

Vol. 12, No. 1

PU.1 Recruits a Second Nuclear Factor to a Site Important for Immunoglobulin κ 3′ Enhancer Activity

JAGAN M. R. PONGUBALA,[1] SUJATHA NAGULAPALLI,[1] MICHAEL J. KLEMSZ,[2] SCOTT R. McKERCHER,[2] RICHARD A. MAKI,[2] AND MICHAEL L. ATCHISON[1]*

Department of Animal Biology, University of Pennsylvania School of Veterinary Medicine, 3800 Spruce Street, Philadelphia, Pennsylvania 19104-6048,[1] and Cancer Research Center, La Jolla Cancer Research Foundation, La Jolla, California 92037[2]

Received 2 August 1991/Accepted 18 October 1991

PU.1 is a B-cell- and macrophage-specific transcription factor. By an electrophoretic mobility shift assay and dimethyl sulfate methylation interference assays, we show that PU.1 binds to DNA sequences within the immunoglobulin κ 3′ enhancer (κE3′). Binding of PU.1 to the κE3′ enhancer assists the binding of a second tissue-restricted factor, NF-EM5, to an adjacent site. Binding of NF-EM5 to κE3′ DNA sequences requires protein-protein interaction with PU.1 as well as specific protein-DNA interactions. This is the first known instance of PU.1 interacting with another cellular protein. NF-EM5 does not cofractionate with PU.1, suggesting that it is a distinct protein and is not a posttranslational modification of PU.1. UV-crosslinking studies and elution from sodium dodecyl sulfate-polyacrylamide gels indicate that NF-EM5 is a protein of approximately 46 kDa. Site-directed mutagenesis studies of the PU.1- and EM5-binding sites indicate that these sites play important roles in κE3′ enhancer activity. By using a series of PU.1 deletion constructs, we have identified a region in PU.1 that is necessary for interaction with NF-EM5. This segment encompasses a 43-amino-acid region with PEST sequence homology, i.e., one that is rich in proline (P), glutamic acid (E), serine (S), and threonine (T).

Transcription factors are composed of at least two functional domains: a DNA-binding domain and a transcriptional-activation domain (29, 35). Characterization of DNA-binding domains has proceeded rapidly. Several major groups which include zinc finger domains, homeodomains, and basic region domains have been identified (9, 20, 29). The mechanisms by which activation domains stimulate transcription are presently unclear. There is, however, some evidence that activation domains may interact with TATA-binding factor TF-IID or TFIIB or with coactivator proteins (4, 18, 24, 25, 36, 40).

In addition to DNA-binding and transcriptional-activation domains, some transcription factors have dimerization or protein-protein oligomerization domains. Thus far, the two best-characterized dimerization domains are the leucine zipper (23) and the helix-loop-helix (HLH) (30) domains. Proteins with these two classes of domains are able to form hetero- or homodimeric complexes (6, 21, 23, 30, 31, 42, 43). These dimerization domains apparently facilitate the correct positioning of amino acid residues necessary for sequence-specific recognition of DNA, and the presence of these domains in transcription factors can greatly influence transcriptional activity. For instance, DNA-binding specificities may be altered by the combinatorial assortment of potential dimerization partners present within a particular cell. Indeed, the HLH-type proteins can be either active or inactive depending on their dimerization partner. Thus, mammalian muscle differentiation and the *Drosophila* sensory organ patterning pathways can be greatly influenced by the presence of certain HLH dimerization partners (3, 8, 10). A similar type of regulation may occur between leucine zipper as well as homeodomain proteins (2, 32, 41). In the above examples, protein-protein interactions are utilized to influence DNA binding. Protein-protein interactions between transcription factors need not always require protein-DNA interactions between both proteins in the complex (22, 26). Elucidation of the mechanisms by which transcription factors interact is important for understanding transcriptional control and ultimately differentiation.

Recently, we cloned a transcription factor, PU.1, from a macrophage cDNA library (19). PU.1 is present in B-lymphoid cells and macrophages and binds to a purine-rich sequence that contains a central core with the sequence 5′-GGAA-3′. PU.1 is known to bind to this sequence in the simian virus 40 (SV40) enhancer. The PU.1 protein sequence is identical to the Spi-1 oncogene sequence (12, 33). Spi-1 appears to be directly involved in the genesis of erythroleukemia induced by spleen focus-forming virus. PU.1 contains several domains identified either functionally or through sequence homology. The DNA-binding domain which is located near the carboxy terminus is homologous to the *ets* family of DNA-binding proteins and is rich in basic amino acids (19). The transcriptional activation domain lies near the amino terminus and is rich in acidic residues (18a, 19). In addition, PU.1 contains a region spanning residues 121 to 159 that is rich in proline (P), glutamic acid (E), serine (S), and threonine (T). Regions rich in these amino acids have been denoted PEST regions, and they may be involved in degradation of intracellular proteins (37). PU.1 does not contain sequences homologous to known dimerization domains (leucine zipper and HLH), and thus far there have been no reports of PU.1 interacting with other proteins.

Recently, we functionally characterized an enhancer (κE3′) that lies 8.5 kb downstream of the mouse immunoglobulin κ constant region exon (34). This enhancer was originally identified by Meyer and Neuberger (27). The κE3′ enhancer contains a 132-bp core that retains nearly full activity in plasmacytoma cells (28, 34). Within this 132-bp core, there are at least two functional elements that have

* Corresponding author.

been mapped to two 25-bp oligonucleotides (oligonucleotides 5 and 7) (34). One of these oligonucleotides (oligonucleotide 5) contains a sequence that resembles the PU.1-binding site. Therefore, we decided to investigate the ability of PU.1 to bind to the κE3′ enhancer.

We report here that the PU.1 protein does indeed bind to DNA sequences present in the κE3′ enhancer. Adjacent to the PU.1-binding site, we have identified an additional DNA motif (EM5) that binds to a nuclear factor (NF-EM5). NF-EM5 is a tissue-restricted 46-kDa protein. The binding of NF-EM5 to DNA requires protein-protein interaction with adjacently bound PU.1. We have localized a region in PU.1 necessary for this protein-protein interaction to a 43-amino-acid segment encompassing the PEST domain. We demonstrate by site-directed mutagenesis studies that both the PU.1-binding site and the EM5 motif play major roles in κE3′ enhancer function.

MATERIALS AND METHODS

Plasmid construction, in vitro transcription, and translation. Clones m5.1 through m5.8 were generated by cloning the appropriate oligonucleotides into the *Bam*HI-*Bgl*II sites of plasmid LBKΔ44. Four head-to-tail copies of each sequence were generated as described previously (34). Each multimerized segment was then transferred to the *Bam*HI site of plasmid TKCAT. The PU.1 plasmids used for in vitro translation were generated from the full-length PU.1 cDNA inserted into the KS+ vector (Stratagene). The PU.1 deletion clones used to map the protein-protein interaction domain were made as follows. Clone 1 was generated by digesting the PU.1 cDNA with *Nsi*I and linking this fragment to a double-stranded oligonucleotide containing an ATG and an *Nsi*I site. Clone 2 was generated by digestion of the PU.1 cDNA with *Nsi*I and *Nco*I and then ligation in the presence of a small oligonucleotide complementary to the overhangs generated by these two enzymes. Clone 3 was generated by isolating the *Nci*I fragment, filling in the ends with Klenow polymerase, and cloning the fragment into the *Eco*RV site of the KS+ vector. Clones 4 and 5 were generated by the polymerase chain reaction with primers which code for initiator methionines. Clone 6 was generated by linearizing the PU.1 plasmid with *Pvu*II and then treatment with *Exo*III and mung bean nuclease to blunt-end the deletions. The DNA was digested with *Sma*I to remove the 3′ end of the PU.1 gene, and the plasmid was religated. The ΔPEST clone was generated by overlap extension by using the polymerase chain reaction (16). Two micrograms of linearized cDNA was transcribed in vitro in the presence of RNasin (Promega) by using either the T3 or the T7 RNA polymerases (Stratagene) according to the manufacturer's specifications. After extraction with phenol and phenol-chloroform and precipitation with ethanol, the resulting RNAs were translated in vitro with a rabbit reticulocyte lysate (Promega) according to the manufacturer's specifications.

Cell culture and transfection. S194 cells were grown in Dulbecco's modified Eagle medium supplemented with 10% horse serum (GIBCO) to a density of 5×10^5 cells per ml. Transfections were performed by the DEAE-dextran (Pharmacia) method according to Grosschedl and Baltimore (14), except that treatment with chloroquine diphosphate was omitted. Each transfection contained 4 μg of test plasmid and 1 μg of the β-galactosidase expression plasmid pCH110 (15). Cells were fed after 20 h and harvested at 40 to 44 h, when cell extracts were prepared. Chloramphenicol acetyltransferase (CAT) assays and thin-layer chromatography were performed according to Gorman et al. (13). Relative CAT activities were determined by calculating the ratios of acetylated to unacetylated [^{14}C]chloramphenicol spots from the thin-layer chromatography plate. Transfection efficiencies were normalized to the level of β-galactosidase in each extract.

Electrophoresis mobility shift assays (EMSAs). Nuclear extracts were prepared by the method of Dignam et al. (7) and were incubated with 4,000 cpm of the ^{32}P-end-labeled DNA probes in the presence 3.2 μg of poly(dI-dC) · poly (dI-dC) in 10 mM Tris–50 mM NaCl– 1 mM dithiothreitol (DTT) 1 mM EDTA–5% glycerol (pH 7.4). Unlabeled competitors were added in the quantities indicated in the legends to Fig. 1 and 2. Incubation was carried out at room temperature for 30 min, and then electrophoresis was performed on 4% nondenaturing polyacrylamide gels. Gels were prerun for 30 min. The oligonucleotide probes were SV40 PU.1 (TG AAATAACCTCTGAAAGAGGAACTTGGTTAGGTA) and κE3′ (GATCCCTTTGAGGAACTGAAAACAGAACCTAG ATC).

DMS methylation interference assays. The κE3′ oligonucleotide probe (see above) was cloned into the *Bam*HI-*Bgl*II sites of plasmid LBKΔ44, regenerating each site. The plasmid was linearized with either enzyme, treated with calf intestine alkaline phosphatase (Boehringer), end-labeled with [γ-^{32}P]ATP by polynucleotide kinase (Pharmacia), and recut with the second restriction enzyme. Labeled DNA fragments were purified by polyacrylamide gel electrophoresis (PAGE). Dimethyl sulfate (DMS) assays were performed according to Atchison et al. (1).

UV cross-linking. The top strand of the κE3′ probe (see above) was annealed at its 3′ end with a complementary 10-nucleotide oligonucleotide. The DNA was made double stranded with Klenow polymerase in the presence of BUdr, [α-^{32}P]dATP, dCTP, and dGTP. Binding reactions were performed with the BUdr-substituted probe with either PU.1 alone or PU.1 mixed with S194 nuclear extract. Binding reactions were electrophoresed on a nondenaturing gel and then irradiated for 15 min with UV light (254 nm). Protein-DNA complexes were excised from the gel, electroeluted, precipitated with 4 volumes of acetone, and subjected to sodium dodecyl sulfate (SDS)-PAGE.

Elution of proteins from SDS-polyacrylamide gels. One-hundred micrograms of S194 nuclear extract was run on a 10% SDS–polyacrylamide gel. The gel was cut into 26 slices of 2.5 mm, and proteins were eluted by incubating the slices for 24 h at 22°C in 50 mM Tris (pH 7.4)–0.1 mM EDTA–0.1% SDS–0.5 mM DTT–100 mM NaCl. Twenty micrograms of bovine serum albumin was added to each fraction, and proteins were precipitated by the addition of 5 volumes of acetone at −20°C for 30 min. Pellets were washed with 100% ethanol, dried, and resuspended in 20 mM HEPES (pH 7.9)–0.1 mM EDTA–0.5 mM DTT–0.5 mM phenylmethylsulfonyl fluoride (PMSF)–10% glycerol–0.1% Nonidet P-40.

Fractionation of NF-EM5. S194 nuclear extract was loaded onto a heparin ultragel A4R column (IBF Biotechnics) in 20 mM HEPES (pH 7.9)–100 mM KCl–0.2 mM EDTA–0.5 mM DTT–20% glycerol–0.1 mM (each) PMSF, leupeptin, and pepstatin. Proteins were eluted in the same buffer with stepwise increases of 100 mM KCl up to 0.6 M. Fractions that contained NF-EM5 were pooled, diluted to 50 mM KCl, and loaded onto a DEAE-Sephacel column (Pharmacia). Proteins were eluted from the column with stepwise increases of KCl as described above.

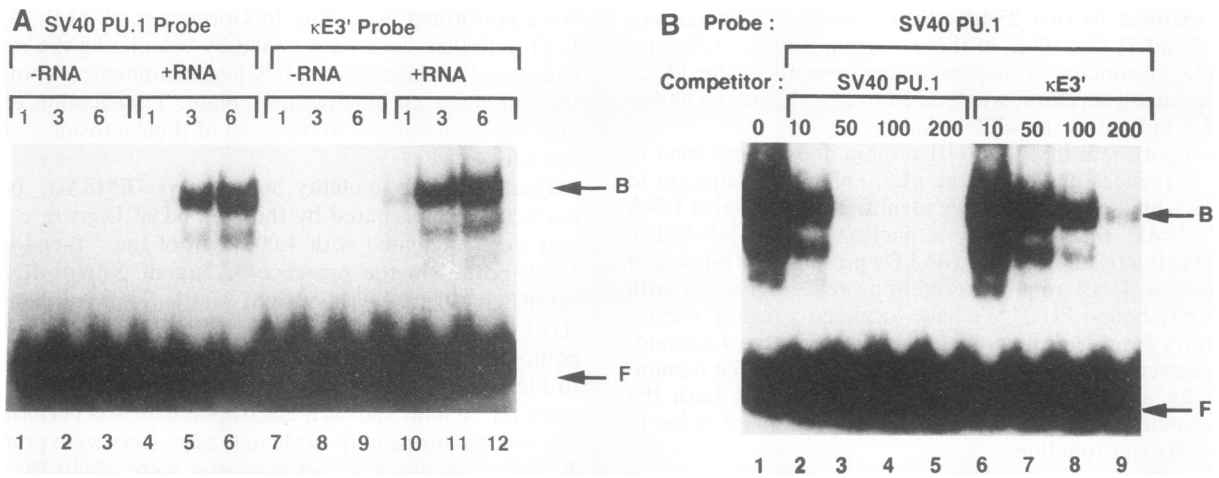

FIG. 1. PU.1 binds to the κE3′ enhancer. (A) κE3′ and SV40 PU.1 probes (see Materials and Methods) were subjected to EMSA with in vitro translation products prepared either with PU.1 RNA (+RNA) or without the addition of RNA (−RNA). The volume (in microliters) of translation product added to each assay is indicated above each lane. (B) Labeled SV40 PU.1 probe was assayed by EMSA with 6 μl of PU.1 prepared by in vitro translation. Unlabeled SV40 PU.1 or κE3′ competitors were added in the amounts (in nanograms) indicated above each lane. Arrows labeled B and F show the positions of the bound and free DNAs, respectively.

RESULTS

PU.1 binds to the κE3′ enhancer. Previously, we determined that a 25-bp oligonucleotide derived from the κE3′ enhancer (oligonucleotide 5) (34) binds to a nuclear(s) factor present in plasmacytoma and pre-B cells. Because this oligonucleotide contains the DNA sequence GAGGAA, which constitutes a PU.1 DNA-binding site, we sought to determine whether PU.1 binds directly to this sequence. The PU.1 protein was prepared by in vitro transcription and translation with the cloned cDNA as the template. The in vitro-translated product was then incubated with ^{32}P-end-labeled oligonucleotide sequences containing either the PU.1-binding site derived from the SV40 enhancer (SV40 PU.1 probe) or the putative site in the κE3′ enhancer (κE3′ probe). Samples were then subjected to the gel EMSA.

As expected, the protein encoded by the PU.1 cDNA bound to the SV40-derived PU.1 DNA sequence (Fig. 1A, lanes 4 to 6). The fainter, higher mobility bands below the bound complex in Fig. 1A are due to internal initiation during translation of the PU.1 mRNA (25a). PU.1 also bound to the κE3′ oligonucleotide probe, yielding a bound complex of identical size (lanes 10 to 12). Therefore, the PU.1 protein is capable of binding to the κE3′ enhancer sequence. No specific binding with either probe was detectable when the in vitro translation reaction was performed without the addition of RNA (lanes 1 to 3 and 7 to 9). To compare the affinity of PU.1 to the SV40 and κE3′ DNA sequences, the bound complex observed with the labeled SV40 probe was inhibited by competition with unlabeled self and κE3′ oligonucleotides (Fig. 1B). Approximately four- to fivefold-more cold κE3′ than the self competitor was required to compete for binding to the SV40-derived probe. Therefore, PU.1 binds more strongly to the SV40 sequence than to the κE3′ sequence.

Identification of a protein that interacts with PU.1 and binds to κE3′ sequences. As presented above, the in vitro-translated PU.1 protein yielded bound complexes of identical mobility when using either the SV40 or the κE3′ oligonucleotide probes. However, comparison of the binding pattern with the κE3′ oligonucleotide probe when using in vitro-translated PU.1 compared with nuclear extract proteins yielded unexpected results. When assayed with nuclear extract proteins, the κE3′ probe produced two bound bands: a fainter band comigrating with the bound band observed with in vitro-translated PU.1 (B1) and an additional more-intense band (B2) of slower mobility (Fig. 2A, lanes 1 and 8). The SV40-derived PU.1 probe did not reveal this more slowly migrating band when assayed with nuclear extract proteins (Fig. 2B). Competition with unlabeled κE3′ oligonucleotide abolished all bound bands (Fig. 2A, lanes 4, 5, 11, and 12), as did the unlabeled SV40 sequences (Fig. 2A, lanes 2, 3, 9, and 10). An unrelated oligonucleotide failed to inhibit the bound complexes (Fig. 2A, lanes 6, 7, 13, and 14). One possible explanation for these results is that the κE3′ probe binds to a second protein present in the nuclear extract in addition to PU.1. The fact that the SV40-derived PU.1-binding site inhibited both complexes observed with the κE3′ probe suggests that this second protein requires PU.1 binding to be detectable in these assays. Therefore, there appears to be a protein-protein interaction between PU.1 and a second protein. We have designated this second protein NF-EM5 (enhancer motif 5, based on its ability to bind to oligonucleotide 5) (34).

To confirm that PU.1 interacts with this second protein (i.e., NF-EM5), which binds to the κE3′ probe, we performed mixing experiments with in vitro-translated PU.1 and nuclear extract proteins. As expected, in vitro-translated PU.1 produced shifted complexes of identical mobility when using the SV40 and κE3′ probes (Fig. 2B, lanes 1 and 4). This complex comigrated with the one observed when the SV40 PU.1 probe was assayed with nuclear extract proteins (lanes 1 and 3). Mixing of PU.1 with nuclear extract proteins did not alter the mobility of this complex with the SV40 probe (lanes 1 to 3). However, with the κE3′ probe, mixture of nuclear extract proteins with in vitro-translated PU.1 caused a significant change in the binding pattern (lanes 4 to 6). In particular, mixture of the in vitro-translated PU.1 with S194 nuclear extract caused a dramatic increase in the intensity of the slower-migrating complex (B2). Complex B2 therefore appears to contain both bound PU.1 and NF-EM5.

To confirm that bands B1 and B2 both contain PU.1, we incubated the in vitro-translated PU.1-nuclear extract mixture with either preimmune or anti-PU.1 serum prior to

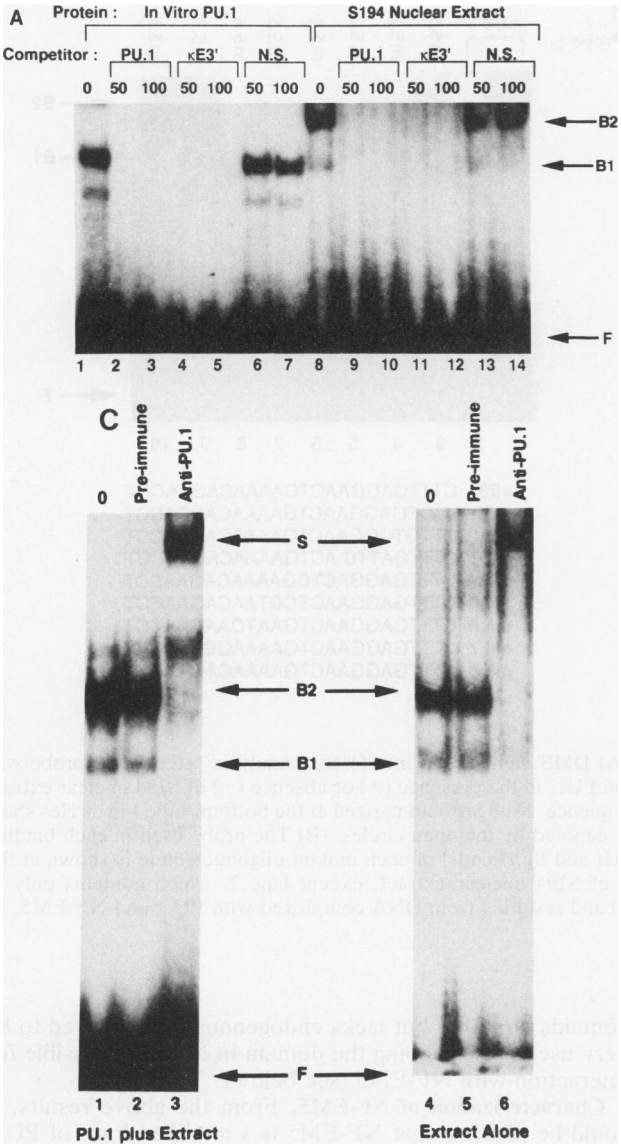

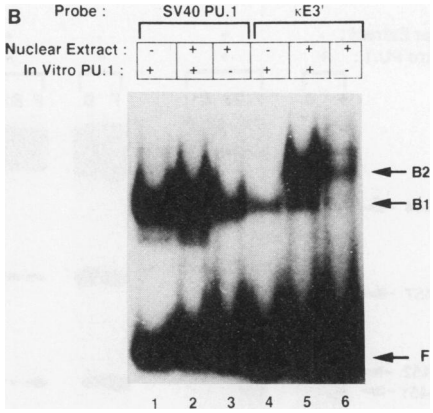

FIG. 2. A second protein interacts with PU.1 and binds to the κE3′ enhancer. (A) κE3′ probe assayed by EMSA with either in vitro-translated PU.1 or 8 μg of plasmacytoma S194 nuclear extract protein. Unlabeled oligonucleotide competitors were added in the quantities (in nanograms) shown above each lane. PU.1, SV40 PU.1 oligonucleotide; κE3′, κE3′ oligonucleotide; N.S., nonspecific oligonucleotide (GATCCACATCTGTTGCTTTCGCTCCCATCCAG ATC) derived from a distinct segment of the κE3′ enhancer. (B) SV40 PU.1 and κE3′ probes subjected to EMSA with in vitro-translated PU.1, S194 nuclear extract (8 μg), or a mixture of PU.1 plus nuclear extract. The presence (+) or absence (−) of PU.1 (2 μl of in vitro translation mix) and S194 nuclear extract is shown above each lane. (C) Lanes 1 to 3, S194 extract (8 μg) plus in vitro-translated PU.1 (2 μl); lanes 4 to 6, S194 extract alone with 1 μl of preimmune (lanes 2 and 5) or anti-PU.1 (lanes 3 and 6) serum prior to EMSA with the κE3′ probe. B1, band resulting from PU.1 binding to either probe; B2, band resulting from PU.1 and NF-EM5 binding to the κE3′ probe; F, free DNA; S, the supershifted complex caused by the anti-PU.1 serum interacting with B1 and B2.

EMSA. Indeed, the anti-PU.1, but not the preimmune serum, caused a supershift in both bands (Fig. 2C, lanes 1 to 3). When nuclear extract alone was assayed (lanes 4 to 6), similar results were observed. Therefore, PU.1 is present in both bound complexes (B1 and B2).

Identification of the PU.1 and NF-EM5 DNA contact points. To more precisely identify the PU.1 and NF-EM5 DNA-binding sites, we performed DMS methylation interference assays. The κE3′ DNA probe was end-labeled on either end and partially methylated with DMS. Binding reactions were performed with in vitro-translated PU.1 protein either alone or in the presence of S194 nuclear extract proteins. Analysis of the κE3′ top strand with PU.1 protein alone indicated that methylation of guanine residues 449, 451, and 452 (numbering according to reference 27) inhibited binding (Fig. 3A, lanes 1 and 2). On the other hand, methylation of guanines on the bottom strand failed to inhibit binding (lanes 6 and 7). These results are identical to the PU.1-DNA contact points identified by Klemsz et al. (19). When the assay was performed with PU.1 protein plus S194 nuclear extract, the band comigrating with the PU.1 band (B1) produced a methylation interference pattern similar to that of PU.1 alone (lanes 2, 5, 7, and 10). Because the B2 complex contains both PU.1 and NF-EM5, it should reveal protein-DNA contacts in addition to those observed with PU.1 alone. Consistent with this prediction, the B2 band revealed a top strand contact site at guanine 457 in addition to the PU.1 contact sites (lane 4). On the bottom strand, the guanine at position 462 showed weak, but reproducible interference. These data are summarized in the bottom panel of Fig. 3A. These data indicate that the NF-EM5-binding site lies immediately downstream of the PU.1-binding site.

Protein-DNA contact sites were further defined by assaying PU.1 and NF-EM5 binding to various oligonucleotide mutants. The PU.1- and NF-EM5-binding region was scanned with oligonucleotides containing 3-bp mutations (Fig. 3B, bottom). Oligonucleotide mutants m5.7 and m5.8 did not affect either PU.1 or NF-EM5 binding (Fig. 3B, lanes 9 and 10). Mutant m5.1 lowered protein-DNA interaction severalfold (lane 3). Mutant m5.6 abolished NF-EM5 binding but did not influence PU.1 binding (lane 8). Mutants m5.3, m5.4, and m5.5 essentially abolished PU.1 and NF-EM5 binding (lanes 5 to 7). Weak PU.1 binding was observed with mutant m5.2 (lane 4). This weak PU.1 binding also allowed a low level of NF-EM5 binding. These results are consistent with the location of the NF-EM5-binding site defined by the DMS methylation interference data shown in Fig. 3A. As expected, any mutation that disrupted the PU.1-binding site abolished the ability of NF-EM5 to bind to DNA, indicating that NF-EM5 requires adjacently bound PU.1 in order to bind to DNA.

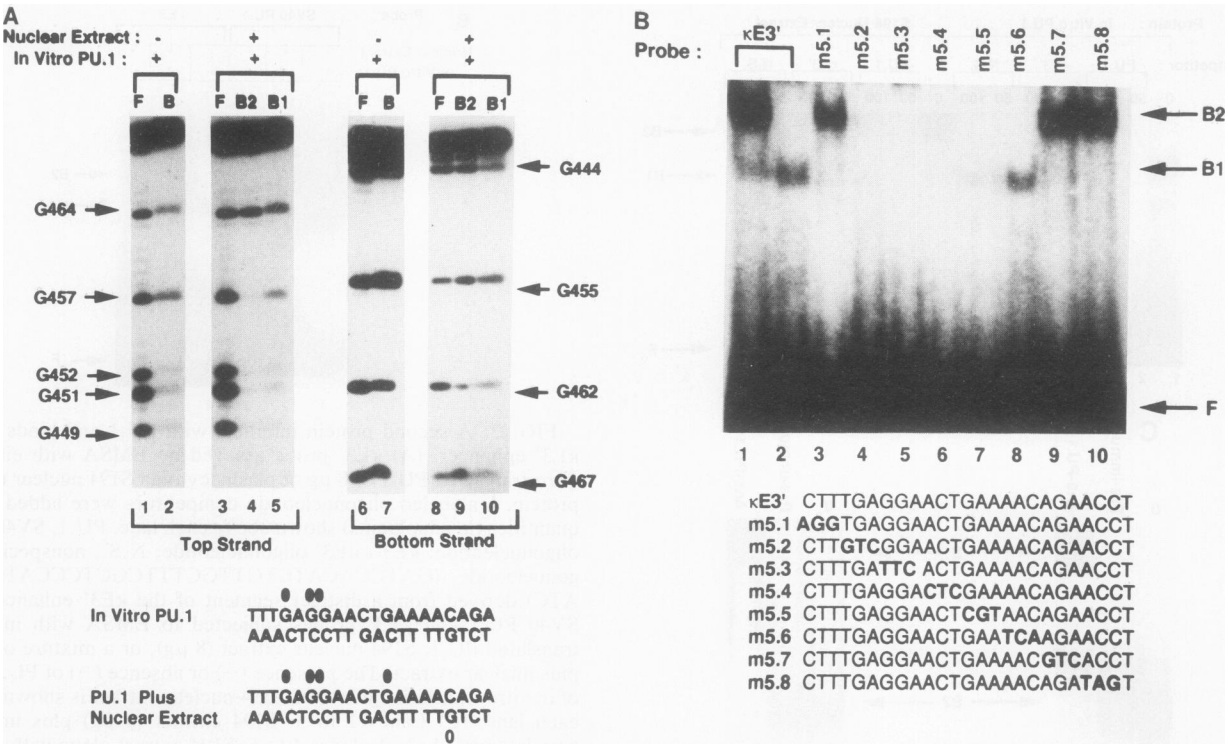

FIG. 3. Identification of DNA contact sites for PU.1 and NF-EM5. (A) DMS methylation interference analysis. κE3′ DNA probe was subjected to DMS methylation interference analysis with in vitro-translated PU.1 in the presence (+) or absence (−) of S194 nuclear extract proteins. Arrows indicate the positions of various G residues in the κE3′ sequence. Data are summarized at the bottom. Filled-in circles show the G residues denoting complete interference, and partial interference is denoted by the open circles. (B) The probe used in each binding assay is shown above each lane, and the DNA sequence (excluding *Bam*HI and *Bgl*II ends) of each mutant oligonucleotide is shown at the bottom. All lanes contained 2 μl of in vitro-translated PU.1 plus 8 μg of S194 nuclear extract, except lane 2, which contains only in vitro-translated PU.1. B1, band resulting from DNA bound to PU.1; B2, band resulting from DNA complexed with PU.1 and NF-EM5; F, free DNA.

NF-EM5 expression is tissue restricted. The κE3′ oligonucleotide probe was assayed with various nuclear extracts either in the absence or presence of in vitro-translated PU.1. Because PU.1 is tissue specific, no binding with non-B-cell nuclear extracts indicative of PU.1 or NF-EM5 would be expected. However, if NF-EM5 is present in these extracts, addition of exogenous PU.1 should yield a PU.1–NF-EM5 complex (B2). The addition of in vitro-translated PU.1 to all B-cell nuclear extracts (3-1 pre-B cells and S194 and Ag8.653 plasmacytoma cells) increased the intensity of the B2 band (Fig. 4, lanes 2 to 7). The great increase in intensity of the B2 band in the S194 and Ag8 lanes suggests that NF-EM5 is present in excess in these extracts. The relatively small increase in B2 observed with the pre-B-cell extract suggests that NF-EM5 may be present in limiting quantities in these cells. In contrast to the assays performed with B-cell extracts, NF-EM5 was undetectable in NIH 3T3, L cell, and COS cell nuclear extracts (lanes 8 to 13). NF-EM5 was also absent from nuclear extracts prepared from two T-cell lines (NCKA and Kvg; data not shown). Therefore, the ability to form the B2 complex is cell type specific.

It should be noted that the B1 and B2 bands were undetectable when the Ag8 extract was assayed alone (Fig. 4, lane 6). The addition of exogenous PU.1, however, revealed the presence of NF-EM5 (lane 7). It is likely that the absence of endogenous PU.1 in this Ag8 extract is due to the relative instability of PU.1 which occurs on extended storage (data not shown). The availability of an extract that contains NF-EM5 but lacks endogenous PU.1 proved to be very useful for mapping the domain in PU.1 responsible for interaction with NF-EM5 (see below).

Characterization of NF-EM5. From the above results, it could be possible that NF-EM5 is a modified form of PU.1 that acquires a new DNA-binding specificity which is revealed in the presence of adjacently bound PU.1. If so, one might expect NF-EM5 to cofractionate with PU.1. S194 nuclear extract was fractionated on heparin-agarose, and each fraction was assayed alone as well as in the presence of in vitro-synthesized PU.1 by the EMSA with the κE3′ probe. Most NF-EM5 eluted from heparin-agarose in 0.2 M KCl (Fig. 5, top). The NF-EM5 in this fraction was incapable of binding to DNA in the absence of exogenous PU.1. Because NF-EM5 did not cofractionate with PU.1, which eluted from the column at higher salt concentrations (data not shown), this suggests, but does not prove, that NF-EM5 is not a modified product of PU.1. However, it is clear that NF-EM5 does not form a strong complex with PU.1 in the absence of its DNA-binding site. The 0.2 M heparin–agarose fractions were pooled and fractionated over DEAE-Sephacel (Fig. 5, bottom). Again, NF-EM5 eluted in the 0.2 M KCl fraction. The presence of NF-EM5 in a single salt fraction after two chromatographic steps suggests that it may be either a single protein or a very stable hetero-oligomer.

To better characterize the protein components in the B2 complex, we performed UV cross-linking studies. A BUdr-substituted κE3′ probe was prepared and assayed by EMSA

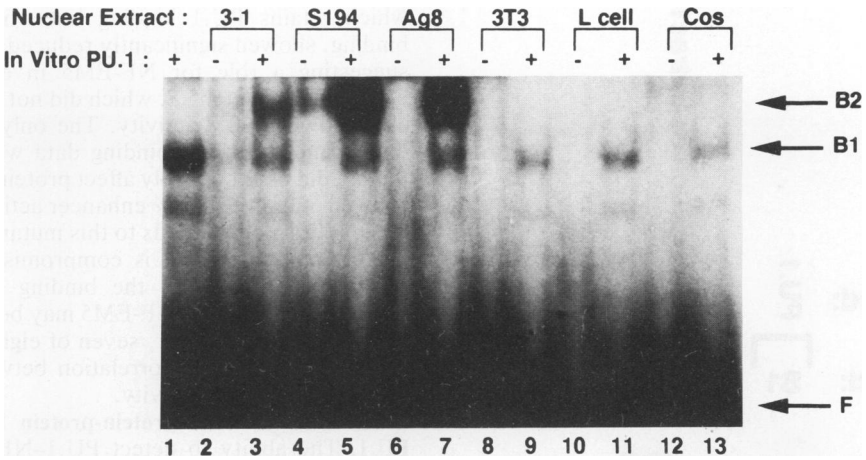

FIG. 4. NF-EM5 is tissue restricted. κE3′ probe was subjected to EMSA with various nuclear extracts in the presence (+) or absence (−) of in vitro-translated PU.1 (2 μl of translation mix). The source of each nuclear extract is indicated above each lane. B1, PU.1 bound to the DNA probe; B2, PU.1 and NF-EM5 bound to the DNA probe; F, free DNA.

with either in vitro-prepared PU.1 alone or PU.1 in combination with nuclear extract protein. After electrophoresis on a nondenaturing gel, the protein-DNA complexes were irradiated in situ with UV light. The B1 and B2 complexes were excised from the gel and then analyzed by SDS-PAGE. PU.1 protein alone yielded a cross-linked protein of approximately 42 kDa (Fig. 6, lane 1, band 1). This is consistent with the mobility of PU.1 estimated by SDS-PAGE (42a). The B1 complex from the PU.1-nuclear extract sample yielded the identical cross-linked product (lane 2). The B2 complex, however, yielded two complexes in addition to the 42-kDa complex; one of 46 and one of 90 kDa (lane 3, bands 2 and 3, respectively). One explanation for these results is that the 46-kDa band represents NF-EM5 and the 90-kDa band represents a cross-linked complex containing both PU.1 and NF-EM5. Alternatively, the B2 complex could consist of PU.1 and two proteins, one of 90 and the other of 46 kDa.

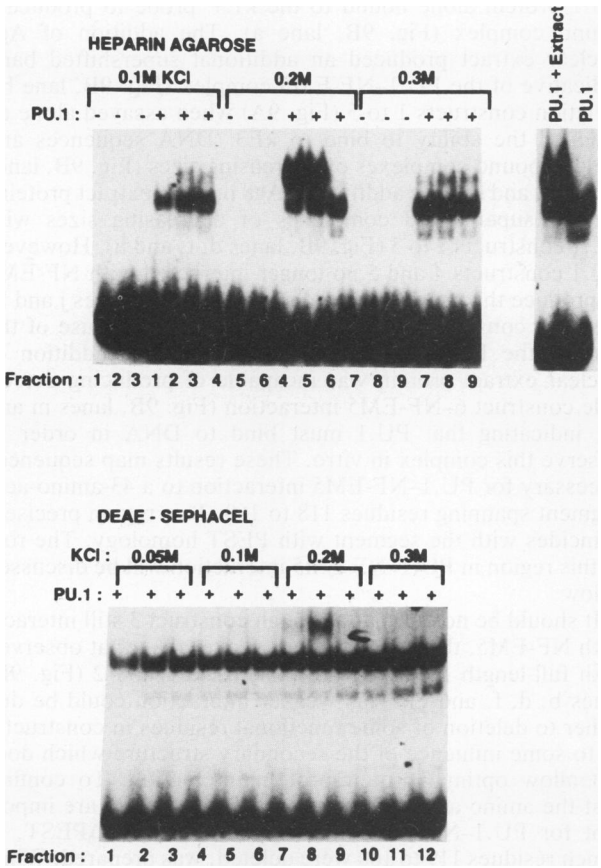

FIG. 5. Partial purification of NF-EM5. Various column fractions were assayed by EMSA with the κE3′ probe in the absence (−) or presence (+) of in vitro-synthesized PU.1. Salt concentrations in each fraction are shown above each lane.

To distinguish between these two possibilities, S194 nuclear extract was fractionated by SDS-PAGE and proteins were eluted from the gel in a total of 26 slices encompassing the 100- to 20-kDa size range. The eluted proteins were assayed by EMSA with the κE3′ probe either alone or in the presence of PU.1. The data from gel slices 5 through 15 are shown. Only proteins that eluted in the 46-kDa size range yielded the B2 complex in the presence of exogenous PU.1 (Fig. 7, fractions 10 and 11). On longer exposures, the endogenous PU.1 protein was clearly evident in fractions 15 and 16. No B2 complex in the 90-kDa range (data not shown) was observed. From the above results, we conclude that NF-EM5 most likely consists of a single polypeptide chain of 46 kDa. However, we cannot exclude the possibility that NF-EM5 binds to DNA either as a homo-oligomer or as a hetero-oligomer with a protein of identical size.

Functional analysis of PU.1 and EM5 DNA-binding sites. Previously, we defined a 132-bp core segment of the κE3′ enhancer that retains most of the enhancer activity observed in plasmacytoma cells. Within this 132-bp segment are at least two functional domains. One of these functional domains (oligonucleotide 5) (34) corresponds to the κE3′ DNA sequences encompassing the PU.1- and EM5-binding sites. To assess the functional activity of each of these binding sites, we prepared DNA constructs with oligonucleotides containing the 3-bp mutations that were assayed for protein binding in Fig. 3B. Each enhancer segment was linked to the herpesvirus thymidine kinase promoter driving expression of the CAT gene. Activity of each DNA construct was measured after transfection into S194 plasmacytoma cells. This

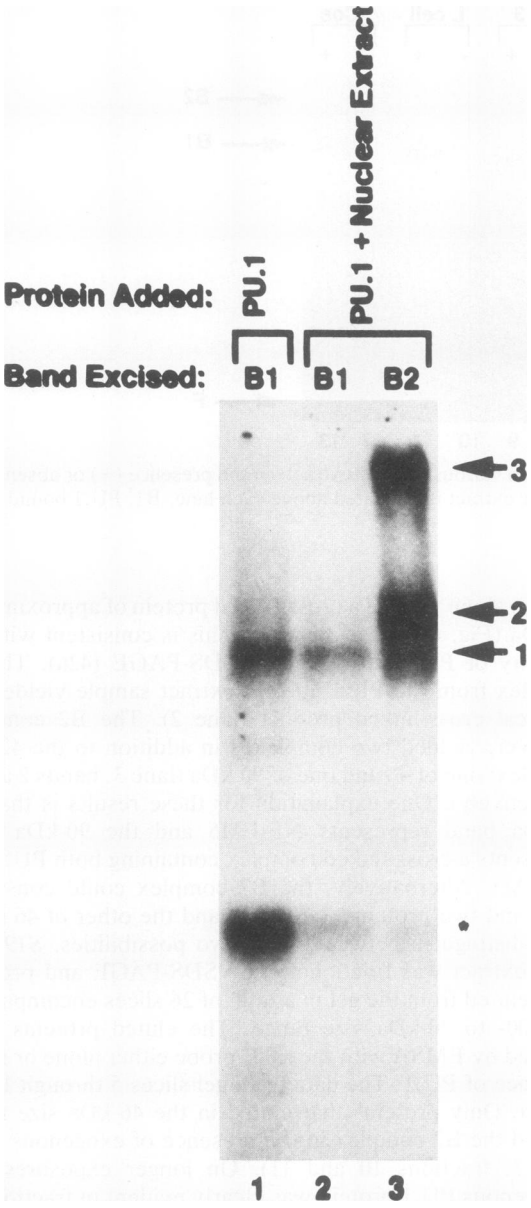

FIG. 6. UV cross-linking analysis of PU.1 and NF-EM5. A BUdr and [α-^{32}P]dATP-substituted κE3′ enhancer probe was analyzed by EMSA with either in vitro-synthesized PU.1 alone (lane 1) or PU.1 plus S194 nuclear extract (lanes 2 and 3). The source of the cross-linked complex is shown above each lane. The positions of cross-linked products are indicated by the numbered arrows. The asterisk denotes a 12-kDa band present in all lanes that is apparently a PU.1 degradation product. The size of each protein was calculated by subtracting 10 kDa contributed by the oligonucleotide probe sequences.

allowed a direct comparison between the binding data in Fig. 3B and transcriptional activity.

Mutation m5.1 which lowered PU.1 and NF-EM5 binding severalfold (Fig. 3B) also showed a fourfold drop in enhancer activity (Fig. 8). The activity of mutant m5.2, which showed only residual PU.1- and NF-EM5-binding activity, also yielded very low transcriptional activity (6.0 and 8.4%). Mutants m5.3, m5.4, and m5.5, which essentially abolished protein binding, lost all enhancer activity. Mutant m5.6, which retains PU.1 binding but which lost all NF-EM5 binding, showed significantly reduced activity (12 and 24%), suggesting a role for NF-EM5 in enhancer activity. As expected, mutant m5.8, which did not affect protein binding, also showed 100% activity. The only construct to show a discrepancy with the binding data was mutant m5.7. This mutant did not noticeably affect protein-DNA interaction but showed only 14 and 21% enhancer activity. It is possible that while NF-EM5 still binds to this mutant sequence, it does so in a configuration that is compromised for transcriptional activity. Alternatively, the binding of additional cellular proteins distinct from NF-EM5 may be influenced by mutant m5.7. In total, however, seven of eight of the 3-bp mutants showed a very close correlation between the binding data and transcriptional activity.

Identification of a protein-protein interaction domain in PU.1. The ability to detect PU.1–NF-EM5 interactions in EMSAs by mixing in vitro-translated PU.1 with nuclear extract proteins (Fig. 2 and 4) afforded us a convenient assay system for mapping the protein domain in PU.1 responsible for this interaction. Seven different PU.1 deletion mutants (Fig. 9A) were transcribed and translated in vitro. These in vitro-synthesized products were then assayed for their ability to bind to DNA and to interact with NF-EM5. Each protein product was assayed with the κE3′ probe by EMSA either alone or in the presence of Ag8 nuclear extract proteins. Because our Ag8 extract does not contain PU.1 (Fig. 4), the only interaction observed should be due to the exogenously added PU.1 protein. As expected, full-length PU.1 protein alone bound to the κE3′ probe to produce a bound complex (Fig. 9B, lane a). The addition of Ag8 nuclear extract produced an additional supershifted band indicative of the PU.1–NF-EM5 complex (Fig. 9B, lane b). Deletion constructs 1 to 5 (Fig. 9A) when assayed alone all retained the ability to bind to κE3′ DNA sequences and yielded bound complexes of decreasing sizes (Fig. 9B, lanes c, e, g, i, and k). The addition of Ag8 nuclear extract proteins yielded supershifted complexes of decreasing sizes with PU.1 constructs 1 to 3 (Fig. 9B, lanes d, f, and h). However, PU.1 constructs 4 and 5 no longer interacted with NF-EM5 to produce the supershifted complex (Fig. 9B, lanes j and l). Deletion construct 6 failed to bind to DNA because of the loss of the PU.1 DNA-binding domain. The addition of nuclear extract protein was incapable of producing detectable construct 6–NF-EM5 interaction (Fig. 9B, lanes m and n), indicating that PU.1 must bind to DNA in order to observe this complex in vitro. These results map sequences necessary for PU.1–NF-EM5 interaction to a 43-amino-acid segment spanning residues 118 to 160. This region precisely coincides with the segment with PEST homology. The role of this region in PU.1–NF-EM5 interaction will be discussed below.

It should be noted that, although construct 3 still interacts with NF-EM5, this interaction is weaker than that observed with full-length PU.1 or with constructs 1 and 2 (Fig. 9B, lanes b, d, f, and g). This weaker interaction could be due either to deletion of some functional residues in construct 3 or to some influence of the secondary structure which does not allow optimal protein-protein interaction. To confirm that the amino acid residues in the PEST region are important for PU.1–NF-EM5 interaction, construct ΔPEST, in which residues 119 to 160 were deleted, was prepared. While this construct still retained DNA-binding ability, it no longer interacted with NF-EM5 (Fig. 9C, lanes 3 and 4). These results confirm that amino acid residues in the PEST region are required for PU.1–NF-EM5 interaction. Although PU.1

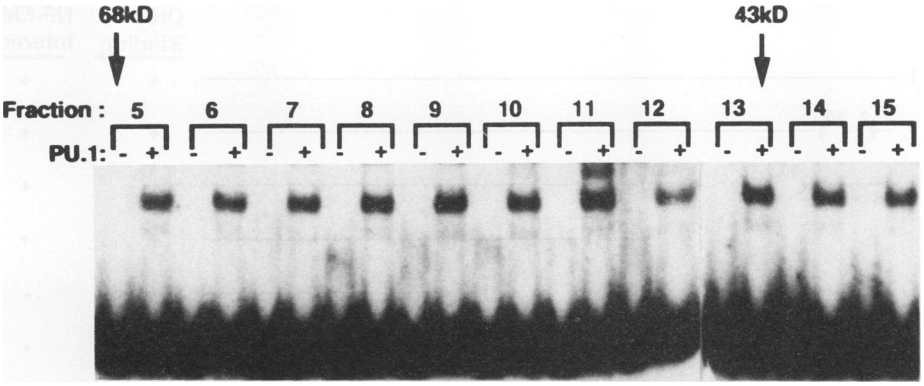

FIG. 7. NF-EM5 elutes from SDS-PAGE in the 46-kDa range. S194 nuclear extract was fractionated on SDS-PAGE. Proteins were eluted from gel slices in the 100- to 20-kDa range and assayed by EMSA with the κE3′ probe for NF-EM5 in the absence (−) or presence (+) of in vitro-translated PU.1. Gel slice numbers are shown above the lanes, and the positions of the 68- and 43-kDa molecular mass markers are indicated.

sequences 119 to 160 are required, we do not know whether they are sufficient to recruit DNA binding by NF-EM5.

DISCUSSION

We have determined that transcription factor PU.1 binds to the κE3′ enhancer. We have also identified a nuclear factor, NF-EM5, that physically interacts with PU.1. This is the first known instance of PU.1 interacting with another protein. Efficient DNA binding by NF-EM5 in vitro requires interaction with adjacently bound PU.1 as well as specific DNA sequences. Thus, binding of NF-EM5 to DNA is undetectable either in the absence of PU.1 binding or when the NF-EM5-binding site is mutated (Fig. 2A, 3B, 5, and 7). NF-EM5 does not cofractionate with PU.1 on heparin-agarose, suggesting that it is not a posttranslational modification of PU.1 and is a distinct protein. However, we cannot exclude the possibility that NF-EM5 is a modified form of PU.1 with altered chromatographic properties. We have determined that NF-EM5 is a 46-kDa protein by both UV cross-linking and by elution from SDS-polyacrylamide gels. The elution of NF-EM5-binding activity from a single size fraction on SDS-PAGE suggests that NF-EM5 is composed of a single polypeptide chain. However, definitive evidence for this point will require further purification or isolation of a cDNA clone encoding NF-EM5.

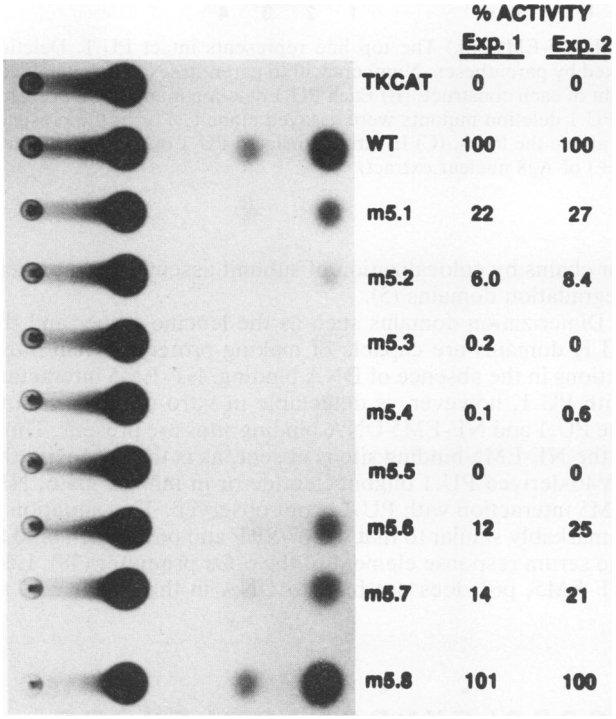

FIG. 8. Transcriptional activity of the 3-bp mutants. Adjacent to each lane is the DNA construct and its relative CAT activity in two experiments in S194 cells. WT, unmutated oligonucleotide 5 sequence (34).

Assays of enhancer activity indicate important roles for the PU.1- and NF-EM5-binding sites in κE3′ enhancer function. It is highly likely that PU.1 and NF-EM5 contribute to enhancer activity in vivo. Transcriptional activity of the 3-bp mutations used to scan the PU.1- and NF-EM5-binding sites correlate well with the protein-binding data (with the exception of mutant m5.7). In addition, the inclusion of anti-PU.1 antiserum in EMSAs resulted in a supershift of all distinct protein-DNA complexes. However, given the complexity of the *ets* family of proteins, we cannot exclude the possibility that other *ets*-related proteins bind to the PU.1 site and contribute to enhancer activity.

PU.1 is primarily expressed in B-lymphoid cells and macrophages. Somewhat surprisingly, NF-EM5 is also restricted in its tissue distribution. While NF-EM5 is present in all B-lymphoid cell lines tested, it is absent in NIH 3T3, L cell, Cos cells, and two T-cell lines. NF-EM5 expression may also be developmentally regulated. The addition of in vitro-translated PU.1 to plasmacytoma nuclear extracts resulted in a very large increase in the supershifted PU.1–NF-EM5 complex, indicating an excess of NF-EM5 in these extracts (Fig. 4). There was, however, a much smaller change in the level of the PU.1–NF-EM5 complex when PU.1 was added to a pre-B-cell extract. This implies that NF-EM5, though present in pre-B cells, may be available in low quantities. The κE3′ enhancer is much more active in plasmacytoma cells than in pre-B cells (28, 34). A developmentally controlled increase in NF-EM5 levels could contribute to this increase in enhancer activity at later developmental stages.

We have mapped a 43-amino-acid region in PU.1 that contains sequences necessary, but not necessarily sufficient,

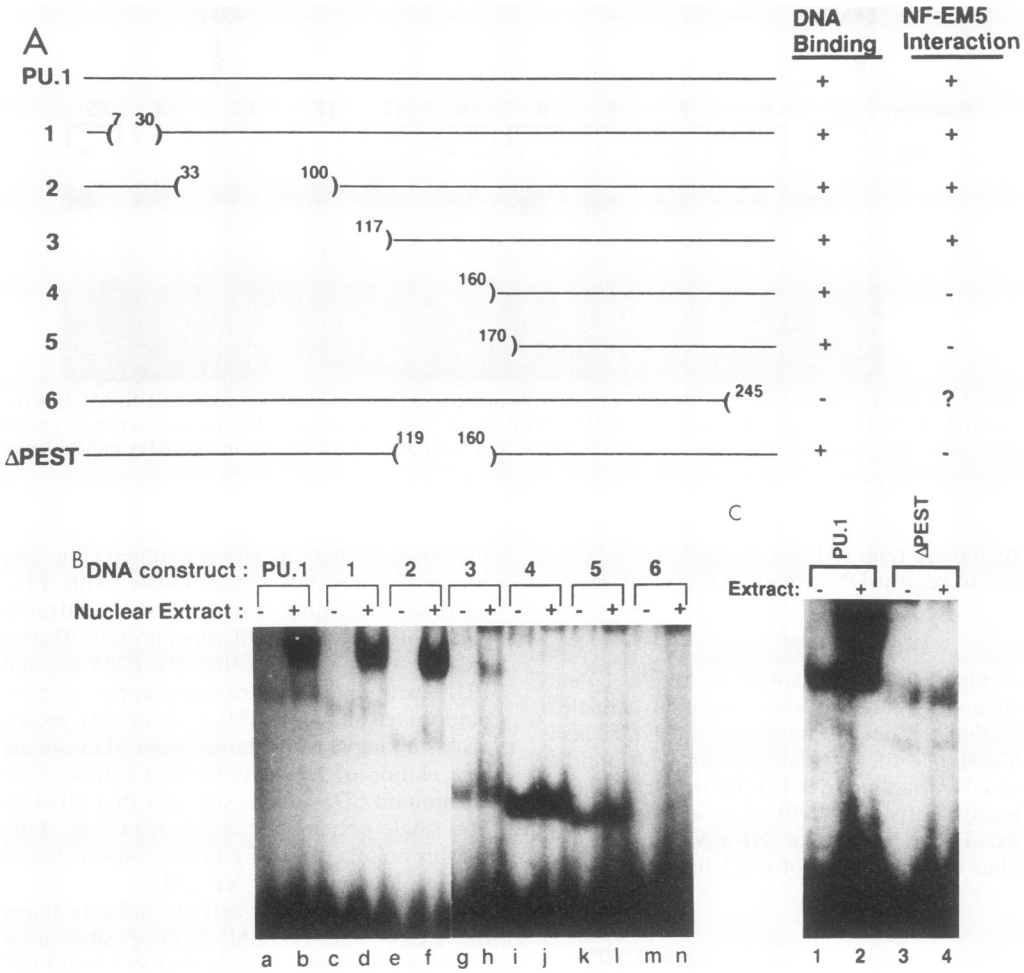

FIG. 9. Identification of PU.1 sequences necessary for interaction with NF-EM5. (A) The top line represents intact PU.1. Deletion mutants 1 to 6 and ΔPEST are diagrammed below. Deleted regions are flanked by parentheses. Numbers within parentheses denote the limits of each deletion. Data obtained in panels B and C are summarized to the right of each construct. (B) Each PU.1 deletion mutant was prepared by in vitro translation and was analyzed by EMSA with the κE3′ probe. PU.1 deletion mutants were assayed alone (−) or in the presence of Ag8 nuclear extract (+). Deletion mutants used in each assay are listed above the lanes. (C) In vitro-translated PU.1 or ΔPEST products were assayed with the κE3′ probe either in the absence (−) or presence (+) of Ag8 nuclear extract.

for interaction with NF-EM5. These sequences are shown in Fig. 10. This corresponds to the region of PU.1 with homology to PEST regions (19). Although little is known concerning PEST regions, they have been implicated in targeting proteins for degradation (37). Whether the PEST region of PU.1 is involved in a similar function is unknown. It is conceivable that protein-protein interactions via the PEST region could simultaneously assist DNA binding as well as protect PU.1 from degradation by masking the PEST region from cellular proteases. If this is true, one might expect PU.1 to be more stable in cells that contain an appropriate oligomerization partner, such as NF-EM5. This is reminiscent of the interesting control exerted on some T-cell receptor chains by colocalization of subunit assembly and protein degradation domains (5).

Dimerization domains such as the leucine zipper and the HLH domains are capable of making protein-protein interactions in the absence of DNA binding. NF-EM5 interaction with PU.1, however, is detectable in vitro only when both the PU.1 and NF-EM5 DNA-binding sites are present. Thus, if the NF-EM5-binding site is absent, as is the case with the SV40-derived PU.1 oligonucleotide or in mutant m5.6, NF-EM5 interaction with PU.1 is not observed. This situation is remarkably similar to that of p67/SRF and p62, which bind to the serum response element of the c-*fos* promoter (38). Like NF-EM5, p62 does not bind to DNA in the absence of an

FIG. 10. Amino acid sequence of the domain responsible for PU.1–NF-EM5 interaction. Asterisks show the location of proline and glycine residues. Acidic (−) and basic (+) residues are also shown.

adjacent binding protein (in this case, p67/SRF). Similarly, the herpesvirus VP16 protein associates with DNA as a complex with Oct-1 as well as other proteins (11). In this case, the interaction between VP16 and Oct-1 requires the Oct-1 homeodomain sequences (17, 22, 39).

The region of PU.1 responsible for protein-protein interaction is unlike presently characterized protein-protein interaction domains. The leucine zipper and HLH protein-protein interactions appear to be due to hydrophobic interactions between amphipathic alpha helices. The region surrounding the PEST segment in PU.1 is unlikely to assume an alpha-helical structure because of its abundance of proline and glycine residues (Fig. 10, asterisks). A more likely mechanism for protein-protein interaction would be a charge-charge interaction. Within the PEST domain, there is a region (residues 134 to 156) in which 10 of 23 amino acids are acidic, with only one basic residue (Fig. 10). Five of six residues between 134 and 139 are acidic. NF-EM5 may interact with this region through a corresponding basic region. This issue can be resolved when NF-EM5 is cloned and characterized.

ACKNOWLEDGMENTS

We thank John Knight for synthesis of some of the oligonucleotides used for plasmid constructions and Y. Hashimoto for T-cell lines NCKA and Kvg. We are grateful to Chuck Van Beveren, Tom Kadesch, and John Burch for helpful comments on the manuscript.

This work was supported by National Institutes of Health grants AI 30656 to R.M. and GM 42415 to M.A. and in part by the Lucille P. Markey Charitable Trust (M.A.) and the Jessie B. Cox Charitable Trust (M.A.).

REFERENCES

1. **Atchison, M. L., V. Delmas, and R. P. Perry.** 1990. A novel upstream element compensates for an ineffectual octamer motif in an immunoglobulin Vκ promoter. EMBO J. **9**:3109–3117.
2. **Auwerx, J., and P. Sassone-Corsi.** 1991. IP-1: a dominant inhibitor of Fos/Jun whose activity is modulated by phosphorylation. Cell **65**:983–993.
3. **Benezra, R., R. L. Davis, D. Lockshon, D. L. Turner, and H. Weintraub.** 1990. The protein Id: a negative regulator of helix-loop-helix DNA binding proteins. Cell **61**:49–59.
4. **Berger, S. L., W. D. Cress, A. Cress, S. J. Triezenberg, and L. Guarente.** 1990. Selective inhibition of activated but not basal transcription by the acidic activation domain of VP16: evidence for transcriptional adaptors. Cell **61**:1199–1208.
5. **Bonifacino, J. S., P. Cosson, and R. D. Klausner.** 1990. Colocalized transmembrane determinants for ER degradation and subunit assembly explain the intracellular fate of TCR chains. Cell **63**:503–513.
6. **Davis, R. L., P.-F. Cheng, A. B. Lassar, and H. Weintraub.** 1990. The MyoD DNA binding domain contains a recognition code for muscle-specific gene activation. Cell **60**:733–746.
7. **Dignam, J. D., R. M. Lebovitz, and R. G. Roeder.** 1983. Accurate transcriptional initiation by RNA polymerase II in a soluble extract from isolated nuclei. Nucleic Acids Res. **11**: 1475–1489.
8. **Ellis, H. M., D. R. Spann, and J. W. Posakony.** 1990. Extramacrochaetae, a negative regulator of sensory organ development in *Drosophila* defines a new class of helix-loop-helix proteins. Cell **61**:27–38.
9. **Evans, R. M., and S. M. Hollenberg.** 1988. Zinc fingers: guilt by association. Cell **52**:1–3.
10. **Garrell, J., and J. Modolell.** 1990. The Drosophila extramacrochaetae locus, an antagonist of proneural genes that, like these genes, encodes a helix-loop-helix protein. Cell **61**:39–48.
11. **Gerster, T., and R. G. Roeder.** 1988. A herpesvirus trans-activating protein interacts with transcription factor OTF-1 and other cellular proteins. Proc. Natl. Acad. Sci. USA **85**:6347–6351.
12. **Goebl, M. G., F. Moreau-Gachelin, D. Ray, P. Tombourin, A. Tavitan, M. J. Klemsz, S. R. McKercher, A. Celada, C. Van Beveren, and R. A. Maki.** 1990. The PU.1 transcription factor is the product of the putative oncogene Spi-1. Cell **61**:1165–1166.
13. **Gorman, C. M., L. F. Moffat, and B. H. Howard.** 1982. Recombinant genomes which express chloramphenicol acetyltransferase in mammalian cells. Mol. Cell. Biol. **2**:1044–1051.
14. **Grosschedl, R., and D. Baltimore.** 1985. Cell-type specificity of immunoglobulin gene expression is regulated by at least three DNA sequence elements. Cell **41**:885–897.
15. **Hall, C. V., P. E. Jacob, G. M. Ringold, and F. Lee.** 1983. Expression and regulation of *Escherichia coli* Lac Z fusions in mammalian cells. J. Mol. Appl. Genet. **2**:101–110.
16. **Ho, S. N., H. D. Hunt, R. M. Horton, J. K. Pullen, and L. R. Pease.** 1989. Site directed mutagenesis by overlap extension using the polymerase chain reaction. Gene **77**:51–59.
17. **Katan, M., A. Haigh, C. P. Verrijzer, P. C. van der Vliet, and P. O'Hare.** 1990. Characterization of a cellular factor which interacts functionally with Oct-1 in the assembly of a multicomponent transcription complex. Nucleic Acids Res. **18**:6871–6880.
18. **Kelleher, R. J., III, P. M. Flanagan, and R. D. Kornberg.** 1990. A novel mediator between activator proteins and the RNA polymerase II transcription apparatus. Cell **61**:1209–1215.

18a. **Klemsz, M.** Unpublished observations.

19. **Klemsz, M. J., S. R. McKercher, A. Celada, C. Van Beveren, and R. Maki.** 1990. The macrophage and B cell-specific transcription factor PU.1 is related to the *ets* oncogene. Cell **61**:113–124.
20. **Klug, A., and D. Rhodes.** 1987. 'Zinc fingers': a novel protein motif for nucleic acid recognition. Trends Biochem. Sci. **12**:464–469.
21. **Kouzarides, T., and E. Ziff.** 1988. The role of the leucine zipper in the fos-jun interaction. Nature (London) **336**:646–651.
22. **Kristie, T. M., and P. A. Sharp.** 1990. Interactions of the Oct-1 POU subdomains with specific DNA sequences and with the HSV α-trans-activator protein. Genes Dev. **4**:2383–2396.
23. **Landschulz, W. H., P. F. Johnson, and S. L. McKnight.** 1988. The leucine zipper protein: a hypothetical structure common to a new class of DNA binding proteins. Science **240**:1759–1764.
24. **Lin, Y.-S., and M. R. Green.** 1991. Mechanism of action of an acidic transcriptional activator in vitro. Cell **64**:971–981.
25. **Liu, F., and M. R. Green.** 1990. A specific member of the ATF transcription factor family can mediate transcription activation by the adenovirus Ela protein. Cell **61**:1217–1224.

25a. **Maki, R. A.** Unpublished observations.

26. **Martin, K. J., J. W. Lillie, and M. R. Green.** 1990. Transcriptional activation by the pseudorabies virus immediate early protein. Genes Dev. **4**:2376–2382.
27. **Meyer, K. B., and M. S. Neuberger.** 1989. The immunoglobulin κ locus contains a second, stronger B-cell-specific enhancer which is located downstream of the constant region. EMBO J. **8**:1959–1964.
28. **Meyer, K. B., M. J. Sharpe, M. A. Surani, and M. S. Neuberger.** 1990. The importance of the 3′-enhancer region in immunoglobulin κ gene expression. Nucleic Acids Res. **18**:5609–5615.
29. **Mitchell, P. J., and R. Tjian.** 1989. Transcriptional regulation in mammalian cells by sequence-specific DNA binding proteins. Science **245**:371–378.
30. **Murre, C., P. S. McCaw, and D. Baltimore.** 1989. A new DNA binding and dimerization motif in immunoglobulin enhancer binding, daughterless, MyoD, and myc proteins. Cell **56**:777–783.
31. **Murre, C., P. S. McCaw, H. Vaessin, M. Caudy, L. Y. Jan, Y. N. Jan, C. V. Cabrera, J. N. Buskin, S. D. Hauschka, A. B. Lassar, H. Weintraub, and D. Baltimore.** 1989. Interactions between heterologous helix-loop-helix proteins generate complexes that bind specifically to a common DNA sequence. Cell **58**:537–544.
32. **Nakabeppu, Y., and D. Nathans.** 1991. A naturally occurring truncated form of FosB that inhibits Fos/Jun transcriptional activity. Cell **64**:751–759.

33. **Paul, R., S. Schuetze, S. L. Kozak, C. A. Kozak, and D. Kabat.** 1991. The Sfpi-1 proviral integration site of Friend erythroleukemia encodes the *ets*-related transcription factor PU.1. J. Virol. **65**:464–467.
34. **Pongubala, J. M. R., and M. L. Atchison.** 1991. Functional characterization of the developmentally controlled immunoglobulin kappa 3′ enhancer: regulation by Id, a repressor of helix-loop-helix transcription factors. Mol. Cell. Biol. **11**:1040–1047.
35. **Ptashne, M.** 1988. How eukaryotic transcriptional activators work. Nature (London) **335**:683–689.
36. **Pugh, B. F., and R. Tjian.** 1990. Mechanism of transcriptional activation by Sp1: evidence for coactivators. Cell **61**:1187–1197.
37. **Rogers, S., R. Wells, and M. Rechsteiner.** 1986. Amino acid sequences common to rapidly degraded proteins: the PEST hypothesis. Science **234**:364–368.
38. **Shaw, P. E., H. Schroter, and A. Nordheim.** 1989. The ability of a ternary complex to form over the serum response element correlates with serum inducibility of the human c-fos promoter. Cell **56**:563–572.
39. **Stern, S., M. Tanaka, and W. Herr.** 1989. The Oct-1 homeodomain directs formation of a multiprotein-DNA complex with HSV transactivator VP16. Nature **341**:624–630.
40. **Stringer, K. F., C. J. Ingles, and J. Greenblatt.** 1990. Direct and selective binding of an acidic transcriptional activation domain to the TATA-box factor TFIID. Nature (London) **345**:783–786.
41. **Treacy, M. N., X. He, and M. G. Rosenfeld.** 1991. I-POU: a POU-domain protein that inhibits neuron-specific gene activation. Nature (London) **350**:577–584.
42. **Turner, R., and R. Tjian.** 1989. Leucine repeats and an adjacent DNA binding domain mediate the formation of functional cFos-cJun heterodimers. Science **243**:1689–1694.

42a. **Van Beveren, C., and R. Maki.** Unpublished results.

43. **Vinson, C. R., P. B. Sigler, and S. L. McKnight.** 1989. Scissors-grip model for DNA recognition by a family of leucine zipper proteins. Science **246**:911–916.